The Sandia Ion-Electron-Optical "Radiation Microscope"

K.M.Horn, B.L.Doyle, D.S.Walsh, and P.E.Dodd
Sandia National Laboratories, Albuquerque, NM, USA, 87185

Abstract

Over the last decade, the ion microbeam facility at Sandia National Labs in Albuquerque has been used to study the effects of ionizing radiation in integrated circuits. Scanned, focused ion beams possess several distinct advantages as a tool for producing controlled single ion exposures of integrated circuit structures. We have increasingly relied upon such measurements as a means of validating simulations of circuits' response to ionizing radiation and pinpointing defects in device design or fabrication. As this experimental tool has evolved from a purely research role toward one that assists in simulation validation and design evaluation, both the experimental hardware and software have also evolved to meet these ends. This work will identify some of the problems dealt with in microbeam-based radiation testing, (e.g. targeting precision, beam damage effects, measurement bandwidth), and their impact on single event upset imaging, charge collection measurement, and verification of charge transport simulations. In describing the design of Sandia's new ion-electron-optical hybrid chamber, we will explain how this design is intended to create a "radiation microscope" whose ease of targeting and impact on the sample can approach the ideally benign nature of an optical microscope.

1. Introduction

1.1 Nuclear Microprobe

Over the last decade, focused, ion microbeams have been used for radiation testing at labs in Japan, Europe, Africa, Australia and the United States. A conceptual rendering of this technique is illustrated in Figure 1. An incident beam of energetic ions is magnetically focused to a sub-micron-sized spot at the surface of a sample. (The world record for the smallest beam spot is held by the University of Melbourne's MicroAnalytical Research Center with a spot size of roughly 50 nm [1].) The focused ion beam can be rastered across a region of the sample or directed to a specific spot. Several different signals arise from the beam-target interaction. As ions impact on the target's surface, electrons are ejected that can be detected and imaged. As ions penetrate into the circuit, they lose energy, creating electron-hole pairs; this is the underlying cause of the observed radiation effects. This charge can also be measured and imaged. Lastly, the effect of this charge on circuit function may also be detected and imaged. Each mode of measurement is described below.

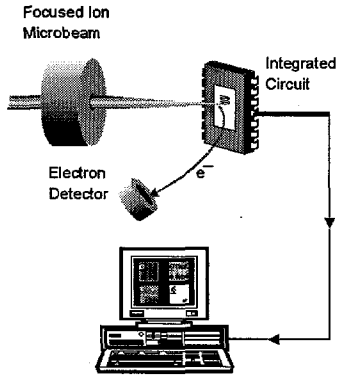

Figure 1. Schematic drawing of microbeam radiation testing.

DISCLAIMER

1.2 Single Event Upset Imaging

In October of 1990, the nuclear microprobe was first used to directly image single event upsets (SEU) in a 16K SRAM fabricated with 1.25 micron technology [2]. Until this application, nuclear microprobes had predominantly been used for analytical measurements of the elemental composition of micron-sized regions of various sorts of targets (biological, mineral, man-made, etc.). In the field of radiation effects, researchers had previously used apertured systems to localize the exposure of integrated circuits (IC) to ionizing radiation [3,4,5]. By focusing rather than aperturing the incident ions, higher ion fluences are readily obtained and it is possible to perform two dimensional scans quickly and with flexible control of the scan area. Upset cross sections can also be measured directly from the upset-image, (such as Figure 2), rather than inferred from the statistics of whole-die exposures. By processing the data live-time, the experimenter can directly image and identify circuit structures susceptible to upset – thus the whole system acts as a sort of *radiation microscope* to "view" upsets and even the charge collection occurring at different circuit structures.

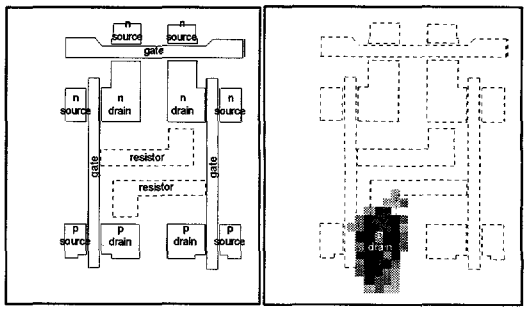

Figure 2. The design mask for a single memory cell of the TA670 16K SRAM is shown next to the corresponding single event upset image recorded using 30 MeV Cu.

The operation of the upset imaging system has been described in detail elsewhere [6]; the salient points are briefly summarized here. Once the ion beam has been focused, the size of the scan is calibrated by imaging TEM (transmission electron microscope) grids of known dimensions and pitch. The full charge generation of the incident ions is then measured in a fully depleted PIN diode whose depletion depth exceeds the range of the incident ion; this step is used to calibrate the charge sensitive pre-amp, amplifier and digitizer for subsequent, quantitative, charge collection measurements. In order to measure the circuit's functional response to the incident ions, two computers act in tandem to record the upset image. One computer controls the positioning of the focused ion beam and the dwell time of the beam at each pixel of the xy-scan; a second computer exercises the target circuit and 'notifies' the first computer whenever a fault is detected. The first computer then records the X and Y position of the beam, the occurrence of the fault, and the elapsed exposure time for the measurement. The resulting data file constitutes an "event file" which records the position and time dependence of each upset occurrence. This event file can be rendered as an upset image, such as shown in Figures 2 and 4.

1.3 Ion Beam Induced Charge Collection (IBICC)

The underlying physical cause of single event upset is the collection of electrical charge at sensitive nodes of the integrated circuit; this charge is produced by creation of electron-hole pairs as the incident ion loses energy penetrating the integrated circuit. Measurements of charge collection using apertured ion exposures were previously done in the 1980's and 90's [7,8,9]. Breese *et al.* first applied scanned, focused ion microbeams to the imaging of charge collection within integrated circuits [10]. This application constitutes another form of *radiation microscopy* for directly viewing charge collection magnitudes within a device in

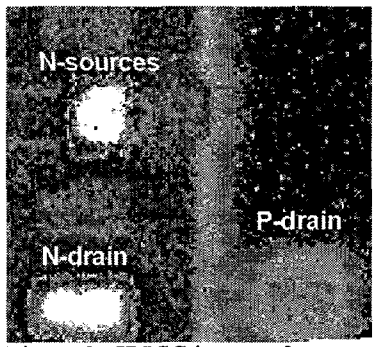

Figure 3. IBICC image of two memory cells in a TA670 16K SRAM.

almost real-time. When combined with SEU-Imaging, these two techniques yield complementary information: how much charge is collected at a specific site AND does that charge cause a circuit malfunction. In the charge collection image shown in Figure 3, (where lighter pixels correspond to higher charge collection), the N-drain and N-sources exhibit the highest charge collection within the memory cell, while from Figure 2 it is seen that it is the p-drain which actually causes circuit upset when exposed to 30 MeV Cu ions.

1.4 Verification of Charge Transport Simulation

It has become increasingly important for designers to be able to predict the radiation response of their circuit designs during the early stages of process development. To this end, three dimensional charge transport simulation codes, such as Davinci [11], are used to predict circuit behavior under irradiation. Verification of these simulation results is achieved with both broad-beam and microbeam testing. In the case of microbeam testing, the controlled, accurate delivery of discrete ions to a specific circuit structure is a nearly perfect experimental replication of the computer simulation conditions. An example of such simulation verification is discussed Section 2.4.

2. Constraints in Radiation Microscopy

2.1 Damage effects during upset imaging

Unlike its optical counterpart, use of the ion microprobe as a radiation microscope is not totally benign. The ions incident on the circuit, which produce the upset or IBICC signals, also produce displacement damage in the device itself. This effect is illustrated in the very initial stages of exposure, shown in Figure 4.

In this instance, the previously unexposed SRAM cell exhibits upsets only in the p-drain during exposure to 30 MeV Cu ions with an LET of 27. (Linear Energy Transfer, or LET, is the amount of energy deposited by the incident ion per unit track length; it is measured in units of MeV/mg/cm^2.) After an exposure of 1200 ions/pixel in this 64x64 pixel scan, the device has been damaged to the extent that ion strikes to the corresponding n-drain of the SRAM cell also begin to produce upsets. This condition also exists in the opposite logic state, as shown in the right-most panel. The dose of 1200 ions/pixel over the 40x40 square micron scan range of this measurement corresponds to a massive 52 Mrad(Si) total dose! This underscores the fact that even using a beam current of only 0.5 fA (~3000 ions/sec), the very small exposure area of the incident beam results in a very large local total dose effect. Consequently, we routinely use ion fluences of only 100 ions/sec or less.

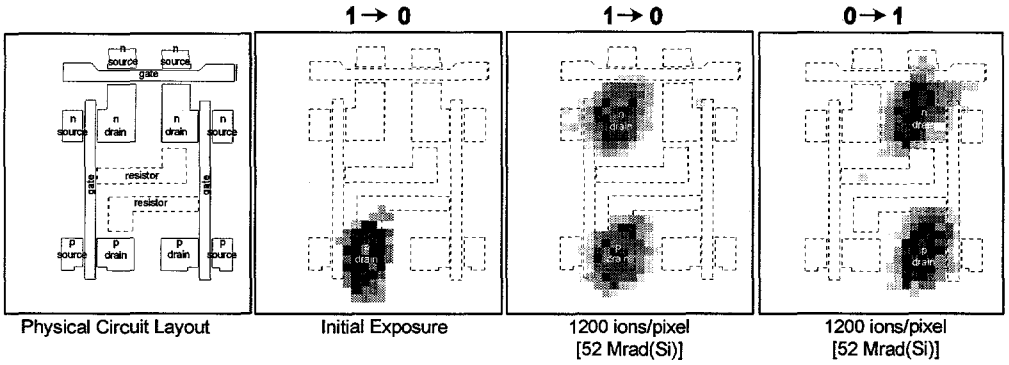

Figure 4. The effects of displacement damage from 30 MeV Cu ions on upset imaging.

Strict control and monitoring of the exposure history of any site is extremely important, since the ion-induced displacement damage resulting from just a few thousand heavy ions can change the number of upsets detected, as illustrated in Figure 5. In this example, an SRAM cell from a TA670 is continuously scanned with a 24 MeV Si beam. After first determining the address of the upsetting cell with the first three scans, the number of upsets per scan is plotted against the scan number over the course of forty scans. During any single scan, the memory cell is repeatedly re-written with the correct value after an upset is detected by the exercising computer, thus each scan across the memory cell can produce multiple upsets. The SRAM cell initially tends toward fewer upsets as the speed of the memory cell slows due to the induced displacement damage. The delivered charge per ion remains the same, but the time constant for its transmission within the cell is increasing, therefore fewer upsets occur. Ultimately, however, the displacement damage within the SRAM cell becomes so great that a fixed logic state is imprinted into the cell and no different value can be written to it. Obviously, this is an extreme example, yet it is important to note that microbeam exposures impart all the incident ions' damage in a very small area and it is therefore vitally important to control and measure the exposure effects from the exposed circuit structure with little, or no, previous ion exposure. This is a key issue in the design of the new Sandia chamber and targeting software.

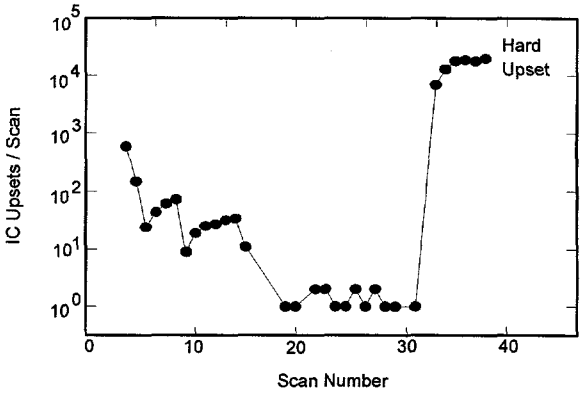

Figure 5. Number of upsets recorded from a single memory cell as a function of scan number. A 24 MeV, 0.5 pA, Si beam focused to a 1μm^2 beam spot produces almost 300,000 Mrad(Si) per 40 x 40 μm scan.

2.2 Damage effects during charge collection imaging

As would be expected, since total dose effects of the incident focused ion beam affect the generation of upsets, it also affects the underlying physical process of charge collection within the structure. Shown in Figure 6 is the IBICC-image recorded from an isolated test FET structure on the 16K SRAM previously shown. The full scan size is 40x40 microns; the p-drain (denoted with the dashed white line in the first and last panels) is 12x5 microns.

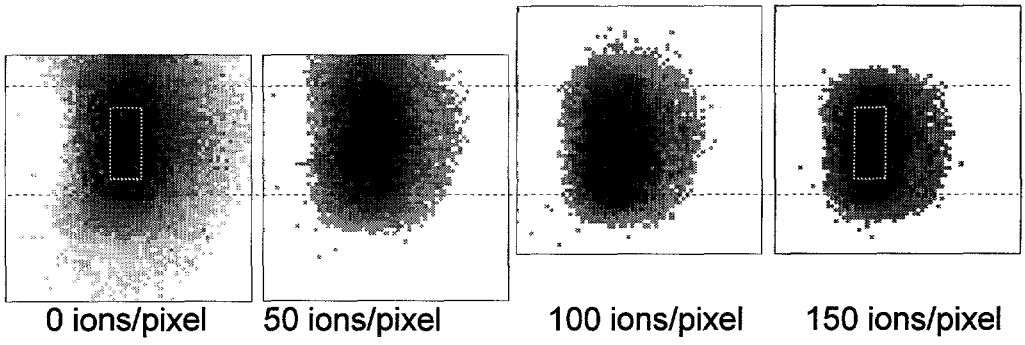

Figure 6. Effects of 14 MeV C displacement damage on charge collection into an isolated FET test structure. The p-drain of the device is outlined in white dashed line in the first and last panels. The p-drain was centered in the scan area after the second panel.

A maximum of 200 14 MeV C ions were delivered to each pixel for the measurement shown in Figure 6. The effect of the accumulated ion damage on charge collection is apparent in the gradual collapse of the region over which charge is collected into the central p-drain. This effect can be successfully modeled as a decrease in the effective diffusion length for charge collection into the drain as displacement damage accumulates over the entire ion exposure area [12].

2.3 Targeting techniques for minimizing pre-measurement damage

Imaging of the target in Sandia's first generation microprobe chamber was initially performed using a secondary electron detector (SED) which collected and amplified the burst of electrons ejected from the target's surface as the ion beam is rastered across the exposure area. Such images (e.g. Figure 7a), were of poor quality owing to the presence of overlying passivation layers on most samples, and also because beam currents and exposure times were necessarily small to avoid the kinds of damage effects described in the previous section.

A more sophisticated application of secondary electron imaging was employed for targeting by the microbeam group at Waseda University [13]. In their system, a secondary electron microscope (SEM) was integrated into the microbeam chamber to permit high quality imaging of the target structure. The improvement in image quality can be compared in Figure 7. However, the SEM's electron beam can also deliver charge into circuit oxides and potentially perturb the circuit's radiation response if the imaging is done prior to the ion exposure.

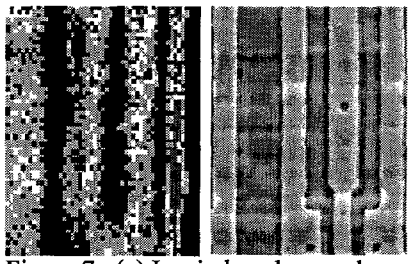

Figure 7. (a) Ion-induced secondary electron image produced by collecting ions emitted by the ions impact with the device surface. (b) corresponding SEM image.

In Sandia's second generation test chamber, (our first chamber designed specifically for radiation testing of integrated circuits), a front-viewing, long working distance, annular-objective, optical microscope, (Jeol SM-OM40 [14]), was incorporated into the targeting chamber; it is also present in the new chamber. This microscope provides selectable magnifications of either 165x, 600x or 930x, with coaxial illumination. Because the ion beam is delivered *through* the light-collecting objective lens, optical targeting is done without the need to reposition the sample for ion microbeam exposure. However, while optical images reveal surface structures of larger dimensions (metallization lines, memory array boundaries, etc.) the ability to resolve features below a few microns is not possible; this capability, however, has increasingly become necessary in probing modern integrated circuits.

In order to selectively target features below the optical resolution limit (which the SEM can do), but NOT alter the device's radiation response before ion exposure (which the SEM, unfortunately, can also do), our latest test chamber employs both optical and SEM imaging methods in conjunction with Raith's ESCOSY GDS II file navigation software and 100 nm resolution translation stage to achieve micron-resolution, no-exposure targeting. GDS II circuit design files are a platform-independent, proprietary file format [15] used to document circuit designs; they are widely used in electron beam lithography and photomask production. In order to accurately navigate around an IC die using the circuit design as a map, SEM images are first recorded from inactive peripheral features on the circuit die, (e.g. unwired test structures, lithographic markings and labels). A three-point alignment of the circuit design to target die is then established which scales and orients the GDS II file to the real-space positioning of the die in its package on the xy-stage. Once this three-point alignment is accurately completed, the die is translated from the SEM to a position beneath the microbeam and coaxial, front-viewing optical microscope. The real-time optical image of

the targeted exposure region is digitally overlain with the scaled and aligned GDS II design, so that visible features such as bit, word, power and ground lines are seen in registry with buried structures such as gates, drains, sources, and resistor diffusions. The ion microbeam scan can then positioned with 0.1 micron precision on the IC die by 'pointing and clicking' on the superimposed optical/GDS II image. Therefore, the SEM in our system serves primarily to scale and rotationally align the target's GDS II design file to the local coordinate axis of the IC die on the stage. The SEM is not used to image electrically active regions of the target. Thus, targeting of the ion microbean exposure site occurs without either ion or electron pre-exposure and is as benign as an optical microscope.

2.4 Measurement Time Resolution

The charge collected from the passage of an energetic ion through an integrated circuit can be divided into a prompt, drift component and a slower, diffusive component. Collection of the prompt charge component can occur up to nanoseconds after the ion strike; the slower, diffusive component can continue over many hundreds of nanoseconds.

A number of factors can lead to the degradation of the charge pulse measured from an IC. Since charge collection pulses are typically measured from either the V_{DD} or V_{SS} lines, significant capacitance is encountered in large-scale integrated circuits. Consequently, loss of all or part of the prompt drift component can occur due to the device itself acting as a low-pass RC filter which may shunt part or all of the high-frequency prompt charge pulse to ground. Further degradation of the fast component of the charge collection signal occurs at bond wire contacts between the die and the IC package, from the package pin to the vacuum electrical feedthrough, and finally in the time response of the charge sensitive pre-amplifier. Obviously the presence of the inherent low-pass RC filter latent in the power network of most commercial devices not fabricated specifically as high-speed test structures is unavoidable.

The effect of this inherent bandwidth limitation in the device itself is illustrated by a set of charge collection measurements performed on p-drains of nearly-identical memory cell designs used in the 16K and 256K versions of SRAMs fabricated using Sandia's CMOS6r process (Figure 8). Three dimensional charge transport calculations, performed using the Davinci simulation package, predict a total collected charge of 255 fC from the p-drain of this design when struck by 20 MeV C. Experimental verification of this result using ion microbeam measurements of the 16K version of this SRAM yields a collected charge of 271 fC - approximately 6% above the simulated value and within the uncertainties of the simulation's prediction and the experiment's accuracy. However, the experimentally measured charge collection from essentially the same memory cell (differing only slightly in overall cell geometry) embedded in a 256K SRAM array is only 123 fC. Since all other experimental variables were held constant, the only significant difference between the 16K and 256K measurements is the increase in the capacitance inherent in the device.

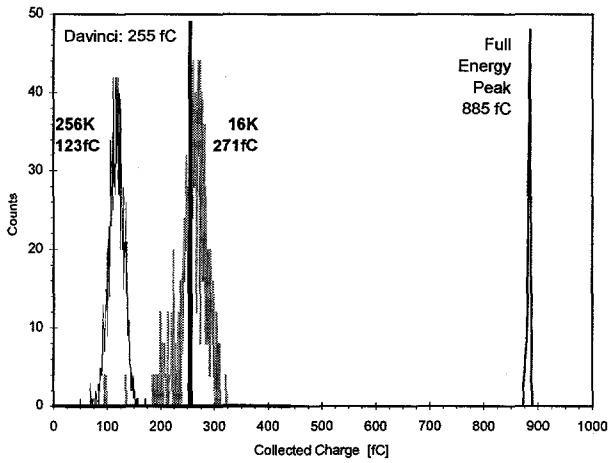

Figure 8. Comparison of the charge collection peaks from 20 MeV Carbon IBICC measurements of 16K and 256K SRAMS of Sandia CMOS6r design and Davinci simulations of this SRAM structure.

In order to measure the faster, prompt charge component directly, a technique called time-resolved ion beam induced charge collection (TRIBICC) is employed [16]. It is possible to accurately measure the prompt charge component with low-capacitance test structures that can be mounted on special copper carriers and the collected signal propagated to an external RF amplifier with a 50 Ω waveguide launcher. Measurements up to 5 GHz analog bandwidth have been performed with ion microbeam exposures on such samples. The design of the new Sandia chamber also supports TRIBICC measurements with SMA feedthroughs and strain-relieved wiring connections to the xy-stage.

Since a circuit's response to ionizing radiation can be dependent on the speed at which it is operated, it can also be necessary to test devices at clock speeds up to several gigahertz. In order to operate at such high speeds it is necessary to place the target device, its support circuitry, and additional testing circuitry on a single board within the vacuum chamber. The current Sandia chamber design accommodates a test board of up to 8"x10".

3. Radiation microscopy chamber

The previous section describes some of the obstacles encountered in microbeam testing. The aim of the design of Sandia's 3rd generation microbeam radiation test chamber has been to: (1) reduce the uncertainty in targeting a specific position of a known circuit structure to less than 0.5 micron, (2) eliminate the need for ANY pre-measurement ion or electron exposure to target circuit structures, and (3) allow sufficient chamber volume to accommodate in-vacuum support circuitry for high speed testing, 8" wafers, or multiple samples.

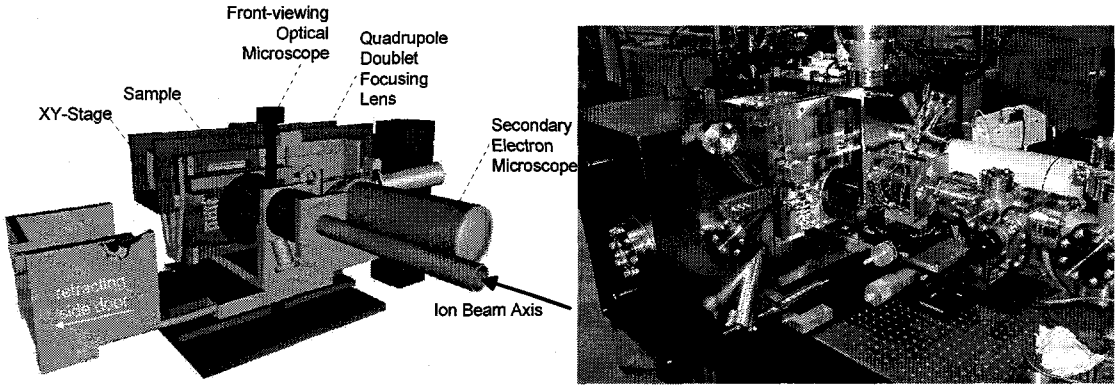

Figure 9. "Cut-away" view and photograph of the installed Sandia "Radiation Microscope" chamber. A wafer, mounted for testing, is visible at the center of the photograph.

The hybrid chamber which achieved these goals was collaboratively designed by Sandia and Raith GmbH, Dortmund Germany [17]. The notable hardware components which support these objectives include:

- 33" x 14½" x 18" vacuum chamber
  - ⇒ internal room for 8" wafer or 8" x 10" circuit board
  - ⇒ target holders supporting DIP, PGA, and wafer mounting
  - ⇒ 150 digital I/O lines
  - ⇒ 10 BNC / SMA feedthrough connectors
- xy-stage with 12" x 4" travel
  - ⇒ 0.1 micron xy positioning precision controlled by laser interferometer
- 2" z-travel of xy-stage
  - ⇒ 5 micron z-translation precision controlled by optical encoders

- FEI/Philips XL series scanning electron microscope – horizontal mount
- JEOL front-viewing, annular objective, long working distance, optical microscope
  $\Rightarrow$ up to 900X magnification
- ESCOSY navigational software package for stage control

4. Conclusion

The use of scanned, focused ion microbeams for radiation testing has proved to be a useful tool in simulation verification and design evaluation of integrated circuits. However, ion microbeam testing techniques also pose a number of potential problems with respect to targeting precision, beam damage effects, and measurement bandwidth. This paper has illustrated these technical obstacles with examples from past microbeam experiments and described the design features of the new Sandia test chamber which have been implemented to mitigate these effects.

Sandia is a multiprogram laboratory operated by Sandia Corporation, a Lockheed Martin Company, for the United States Department of Energy under contract DE-AC04-94AL85000.

References

1. G.F.Bench and G.J.F.Legge, "High Resolution STIM", Nucl. Instrum. And Methods B, vol. 40/41, pp. 655-663, 1989.
2. K.M.Horn, B.L.Doyle, D.S.Walsh and F.W.Sexton, "Application of the Nuclear Microprobe to the Imaging of Single Event Upsets in Integrated Circuits", Scanning Microscopy, Vol. 5, No. 4, 1991, pp. 969-976.
3. A.B.Campbell and A.R.Knudson, "Use of an ion microbeam to study single event upsets in microcircuits," IEEE Trans. Nucl. Sci., vol. NS-28, pp. 4017-4021, 1981.
4. F.J.Henley and W.G.Oldham, "Soft error studies using a scanning source", Proc. 20th IEEE Reliability Physics Symp., 1982, pp.88-91.
5. D.F.Heidel, U.H.Bapst, K.A.Jenkins, L.M.Geppert, and T.H.Zabel, "Ion microbeam radiation system", IEEE Trans. Nucl. Sci., vol. 40, pp.127-134, 1993.
6. K.M.Horn, B.L.Doyle and F..W.Sexton, "Nuclear Microprobe Imaging of Single Event Upsets", IEEE Transactions on Nuclear Science, Vol. 39, No. 1, Feb. 1992, pp. 7-12.
7. A.R.Knudson and A.B.Campbell, "Charge collection Measurements for Energetic Ions in Silicon", IEEE Trans. Nucl. Sci., vol. NS-29, pp.2067-2071, 1982.
8. P.J.McNulty, W.J.Beauvais, D.R.Roth, J.E.Lynch, A.R.Knudson, and W.J.Stapor, "Microbeam analysis of MOS circuits", RADECS 91: First European Conf. On Radiation Effets on Devices and Systems 1991, pp.435-439.
9. T.J.Aton, J.A.Seitchik, S.D.Hantz and H.Shichijo, "Accurate measurements of small charges collected on junctions from alpha particle strikes using an accelerator-produced microbeam", Proc. Intl. Reliability Physics Symp., 1995, pp.303-310.
10. M.B.H.Breese, P.J.C.King, G.W.Grime, and F.Watt, "Microcircuit imaging using an ion-beam induced charge", J.Appl. Phys., vol. 72, no. 6, pp. 2097-2104, 1992.
11. Avant! Corporation, TCAD Business Unit, 46871 Bayside Parkway, Fremont, CA 94538.
12. M.B.H.Breese and K.M.Horn, "The Influence Of Ion Induced Damage On Lateral Charge Collection And IBIC Image Contrast", ", Nucl. Instrum. And Methods B, vol. 138, pp. 1349-1354, 1998.
13. I.Ohdomari, M.Sugimori, M.Koh, K.Noritake, M.Ishikawa, H.Shimizu, R.Tanaka, T.Kamiya, and N. Utsunomiya, "Ion Microprobe System At Waseda University For Semiconductor Analysis", Nucl. Instrum. And Methods B, vol. 54, pp. 71-74, 1991.
14. Jeol USA, Inc. 11 Dearborn Rd. Peabody, MA, USA.
15. Cadence Design Systems, Inc., 2655 Seely Rd., San Jose, CA 95134.
16. H.Schone, D.S.Walsh, F.W.Sexton, B.L.Doyle, J.F.Aurand, P.E.Dodd, R.S.Flores, and N.Wing, "Time-Resolved Ion Beam Induced Charge Collection (TRIBICC) in Micro-Electronics", Nucl. Instrum. And Methods B, vol. 158 pp. 424-431, Sept. 1999.
17. Raith GmbH, Haurt 18 (Technologiepark), D-44227 Dortmund, Germany.